Figures

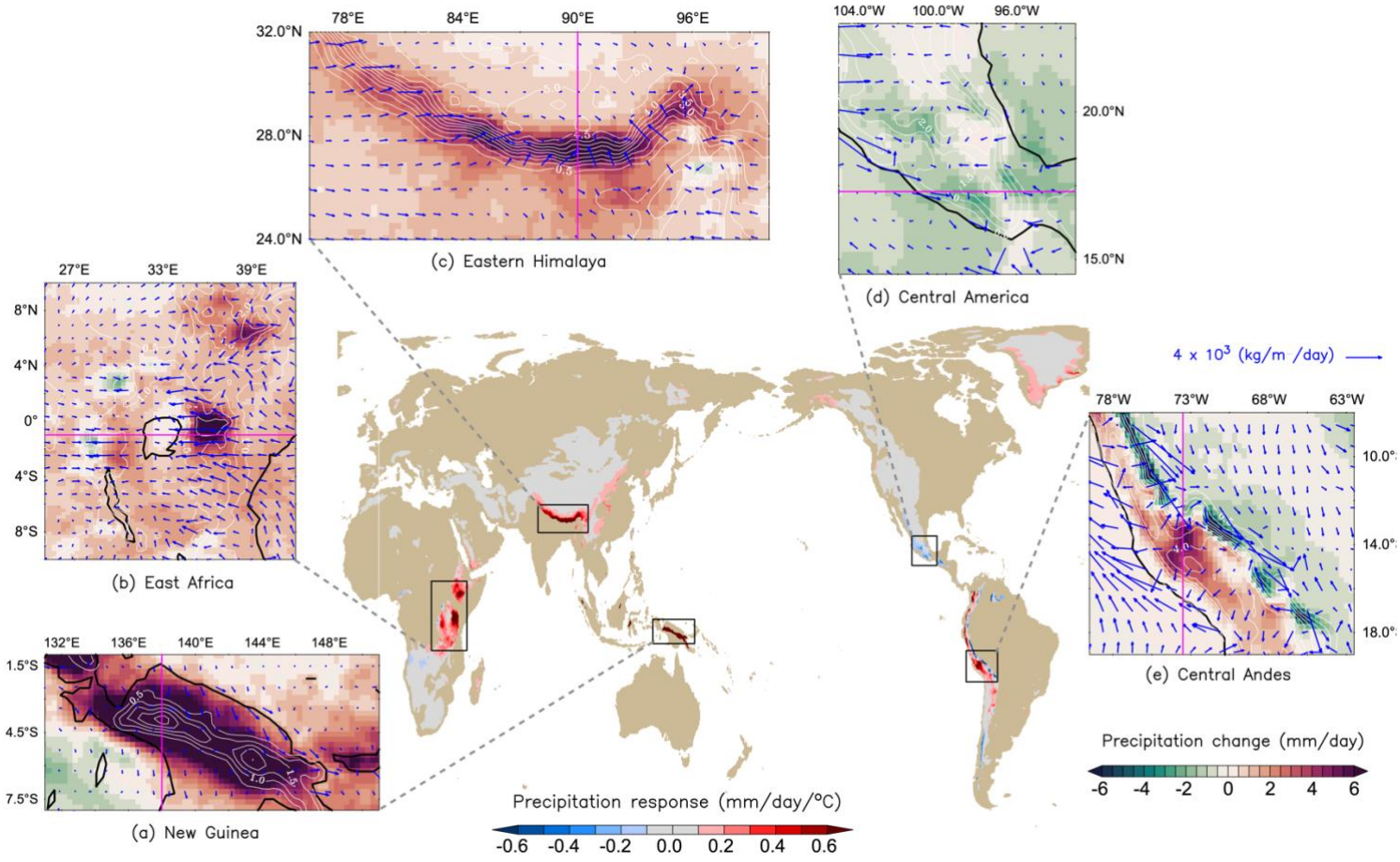

Fig. 1. Projected elevation-dependent precipitation changes over the global mountain in response to 4×CO_2. The center panel indicates precipitation response (absolute change in precipitation rate) to local warming associated with future change. The sub-panels indicate precipitation changes in 4×CO_2 compared to PD over (a) New Guinea, (b) East Africa, (c) Eastern Himalaya, (d) Central America, and (f) Central Andes. The blue vectors are vertically integrated horizontal moisture flux, and the white contour shows an elevation orography of 0.5 km interval. The magenta line indicates either the longitude or latitude of the cross-section for further analysis.

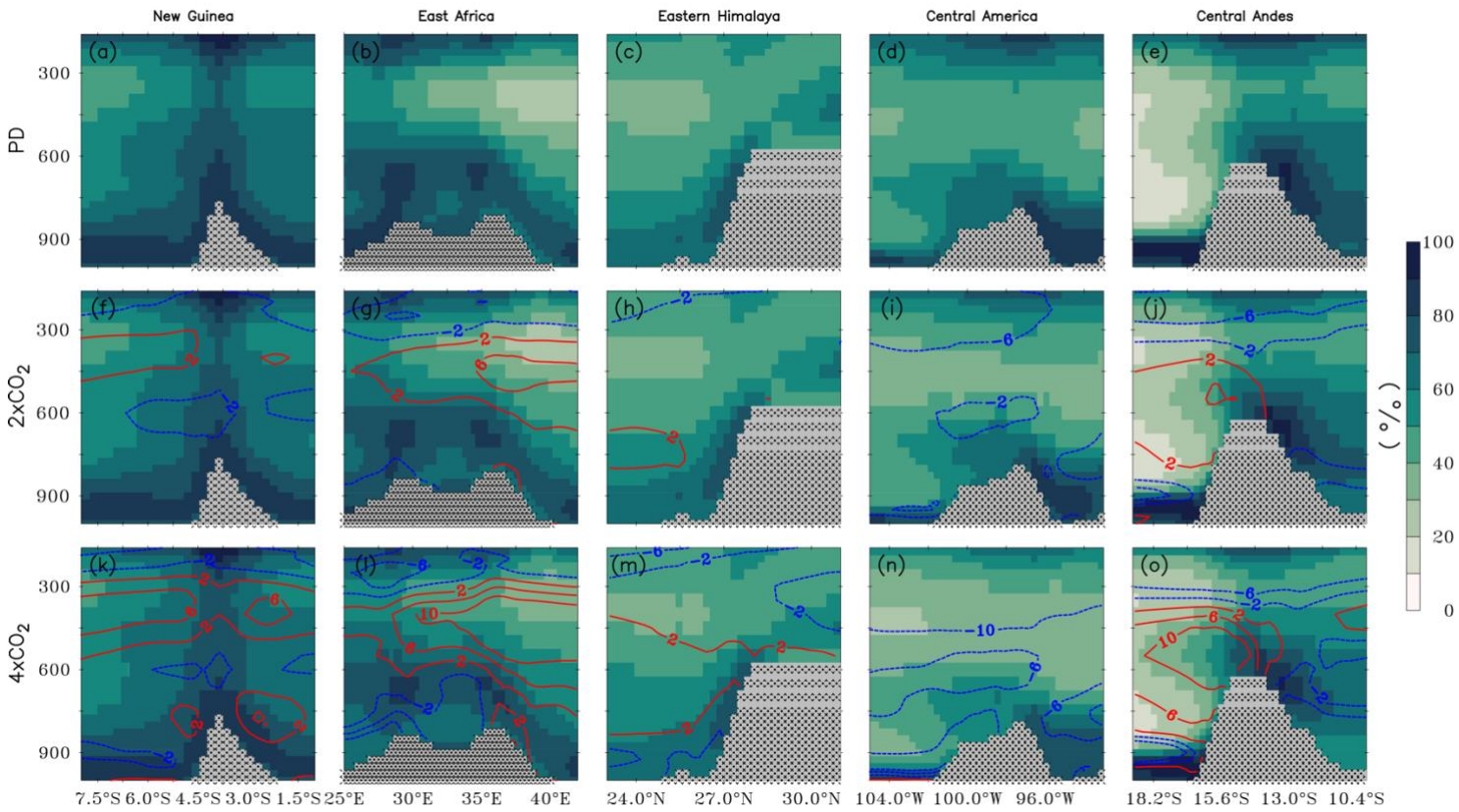

Fig. 2. Vertical structure of relative humidity. Vertical profile of relative humidity (shading) and its anomalies (contour) over New Guinea, East Africa, Eastern Himalaya, Central America, and Central Andes. (a)-(e) For the PD mean state, (f)-(j) for 2×CO_2 mean state, and (k)-(o) for 4×CO_2 mean state respectively. Contours represent relative humidity anomalies due to CO_2 perturbation, where positive values indicate boosts and negative values indicate reduction.

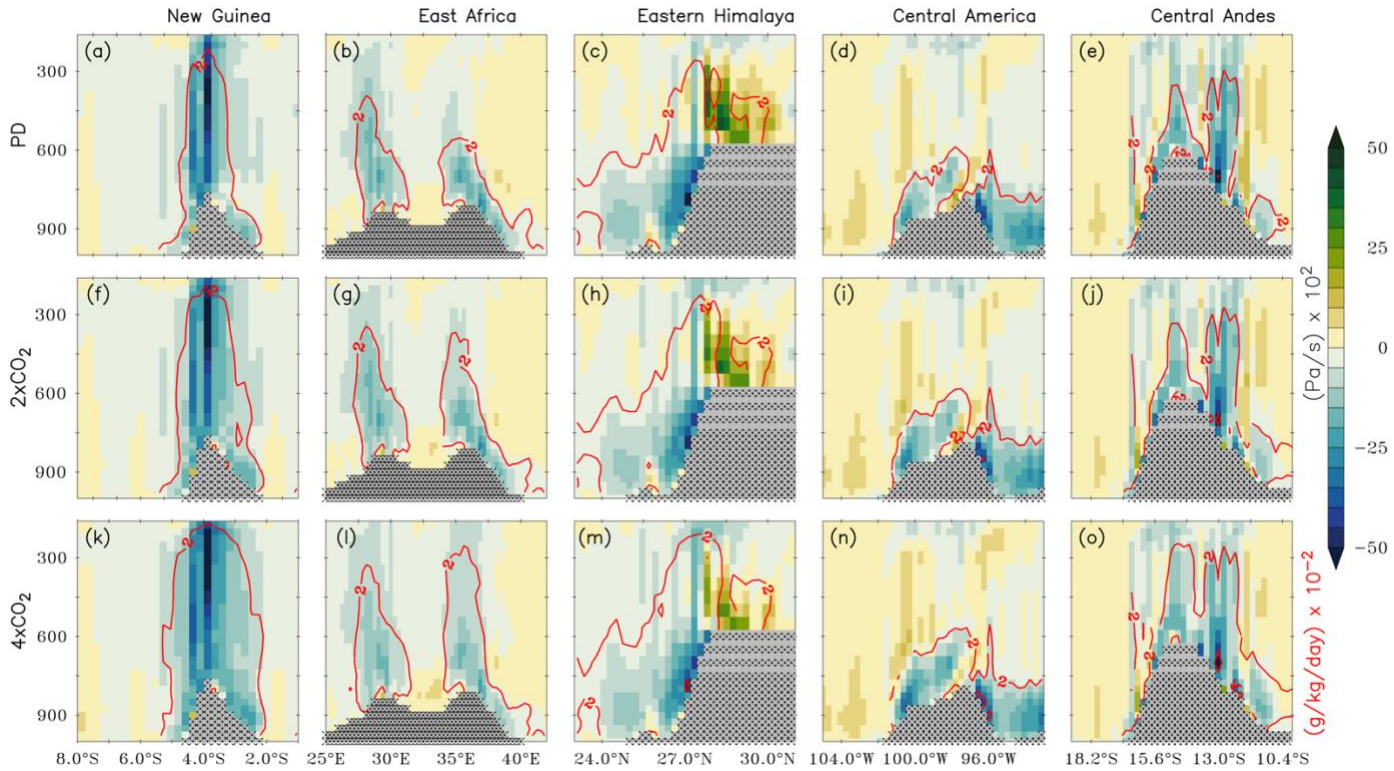

Fig. 3. Vertical structure of vertical velocities with local saturated condensation rate. Vertical profile of mean vertical velocity (shading) and local saturated condensation rate (contour) over New Guinea, East Africa, Eastern Himalaya, Central America, and Central Andes. (a)-(e) PD, (f)-(j) 2×CO_2 experiment, and (k)-(o) 4×CO_2 perturbation experiment respectively. Here, we consider upward motion using the daily scale as precipitation events are associated with upward motions, which offers a clearer idea about ascending motion.

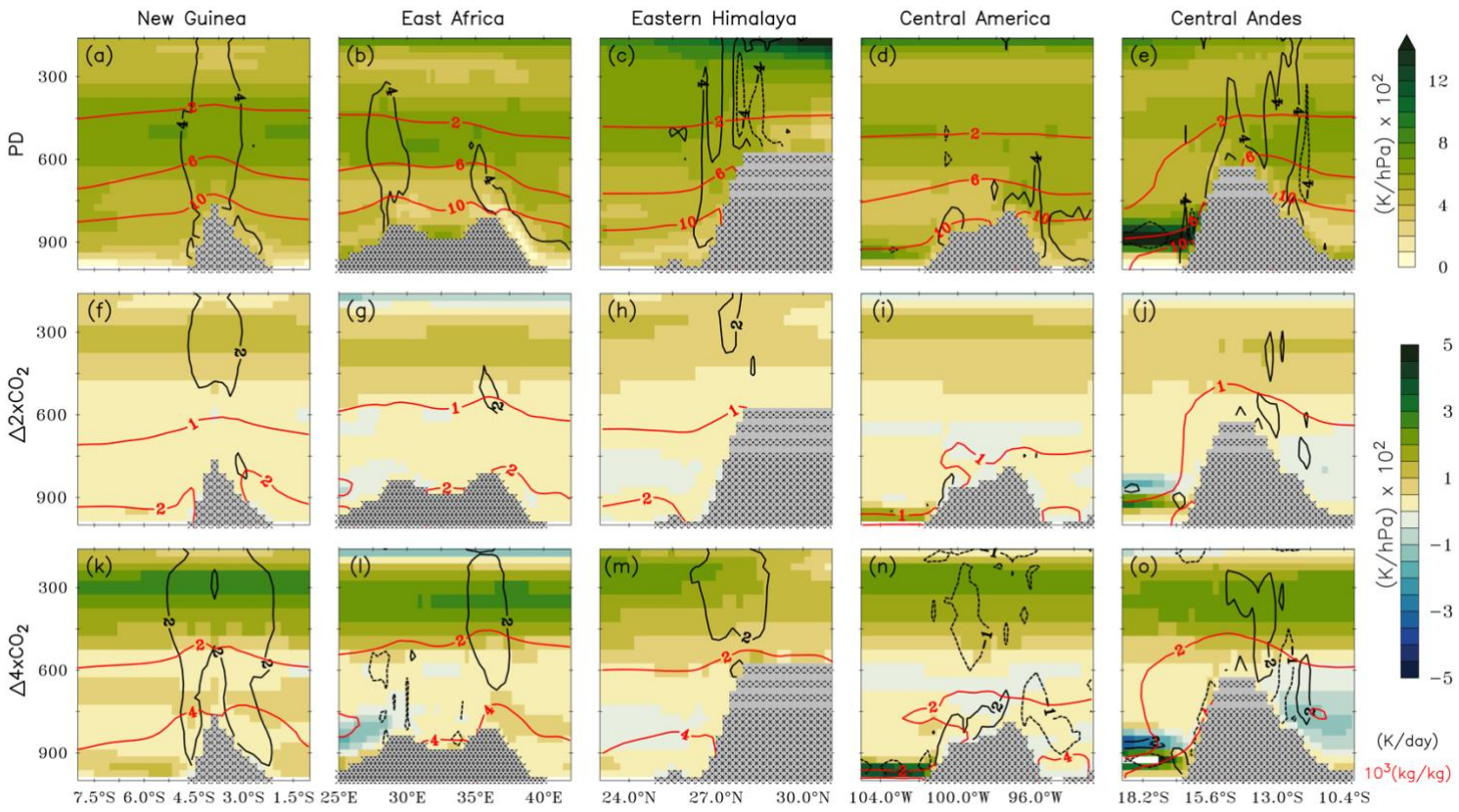

Fig. 4. Vertical structure of thermodynamic condition. Vertical profile of static stability (shading), diabatic heating (black contour) and specific humidity (red contour) over New Guinea, East Africa, Eastern Himalaya, Central America, and Central Andes (a)-(e) for the PD mean state, (f)-(j) for 2×CO_2 anomalies, and (k)-(o) for 4×CO_2 anomalies respectively.

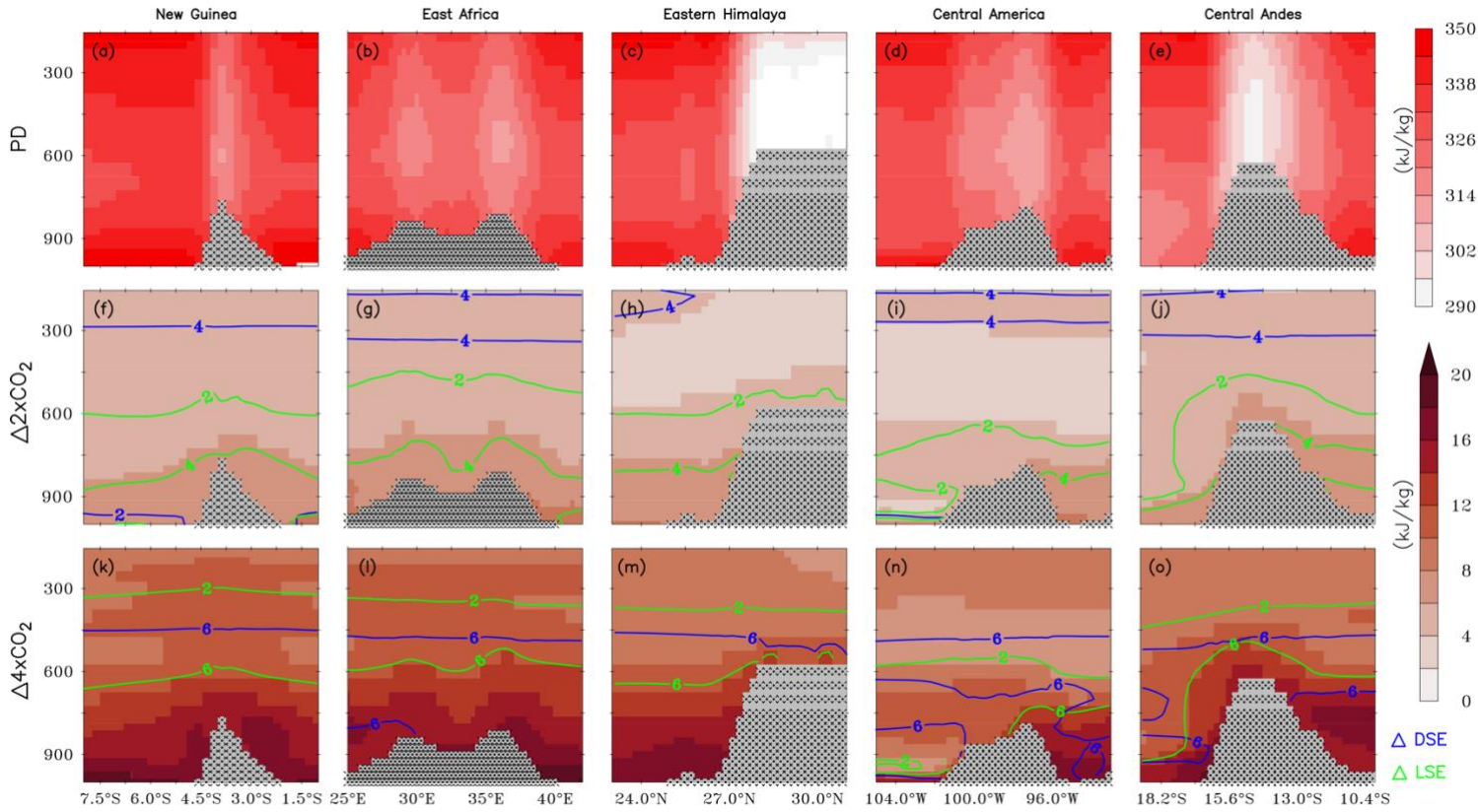

Fig. 5. Vertical structure of moist static energy. Moist static energy (shading) over New Guinea, East Africa, Eastern Himalaya, Central America, and Central Andes for (a)-(e) PD mean state, (f)-(j) 2×CO_2 anomalies, and (k)-(o) 4×CO_2 anomalies. The green color contour represents changes in latent static energy, and the black color contour represents changes in dry static energy.

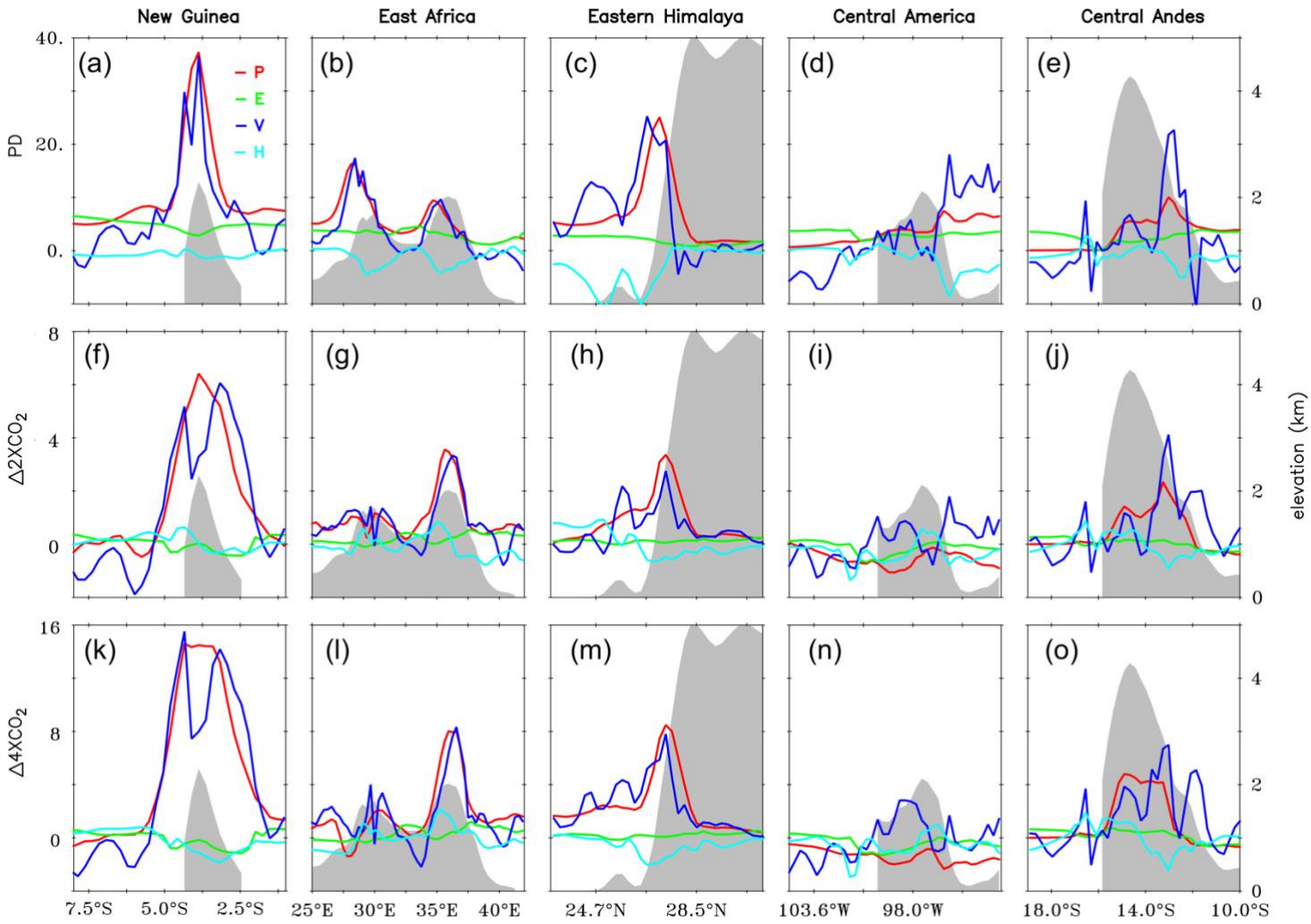

Fig. 6. Moisture budget analysis over selected mountain regions. Cross-section of moisture budget terms (a-e) for PD mean state, (f-j) for $2xCO_2$ anomalies, (k-o) $4xCO_2$ anomalies respectively. The colored lines indicate the mean state of moisture budget terms; red for precipitation (P), green for evaporation (E), blue for vertical moisture advection (V), and cyan for horizontal moisture advection(H). The shaded grey color represents associated elevation orography.

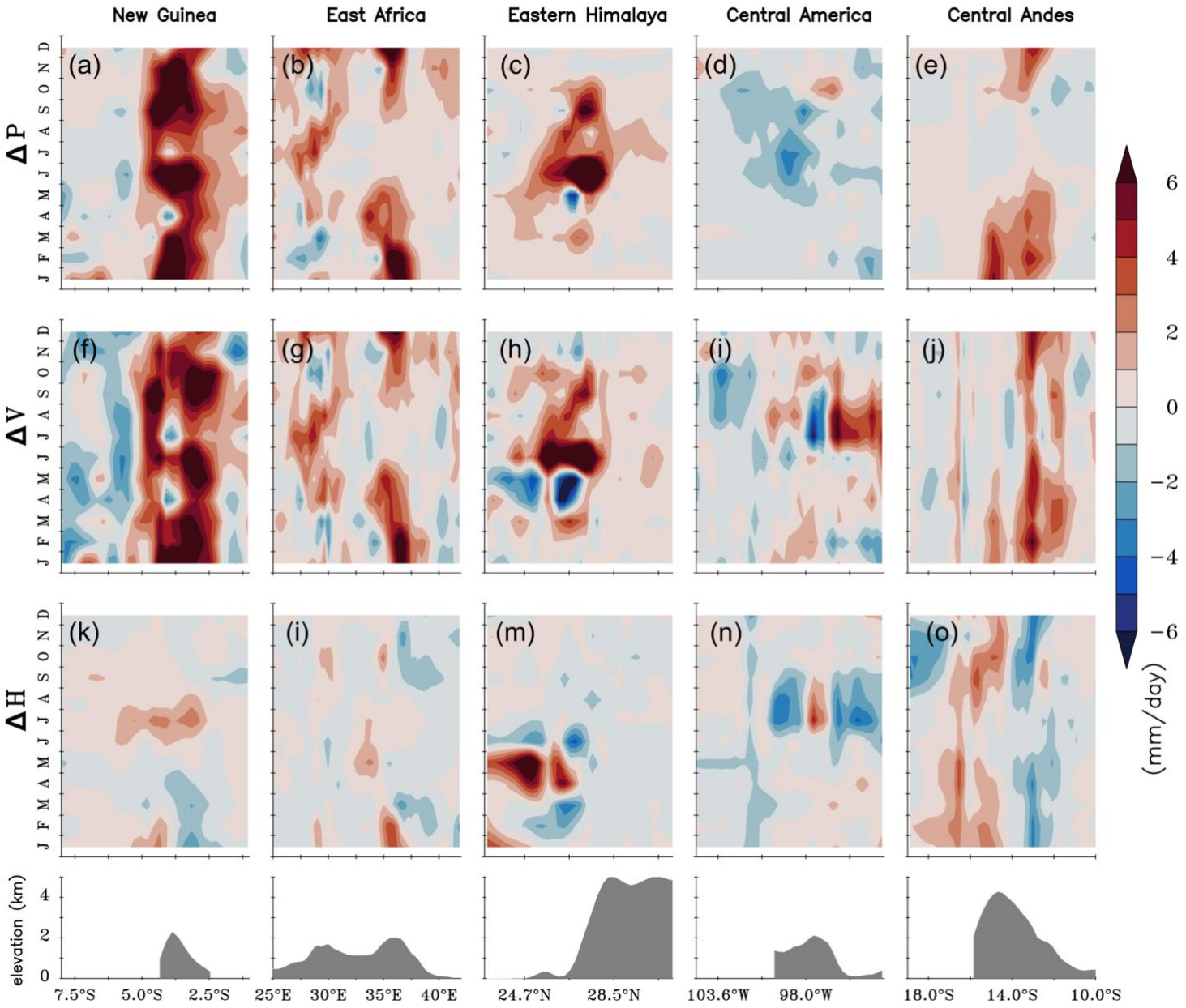

Fig. 7. Seasonal cycle evaluation of dominant terms from moisture budget analysis. Cross-section of moisture budget terms for change in precipitation (P), change in vertical moisture advection (V) and horizontal moisture advection (H) respectively. The shaded grey color in bottom panels represents associated elevation orography.

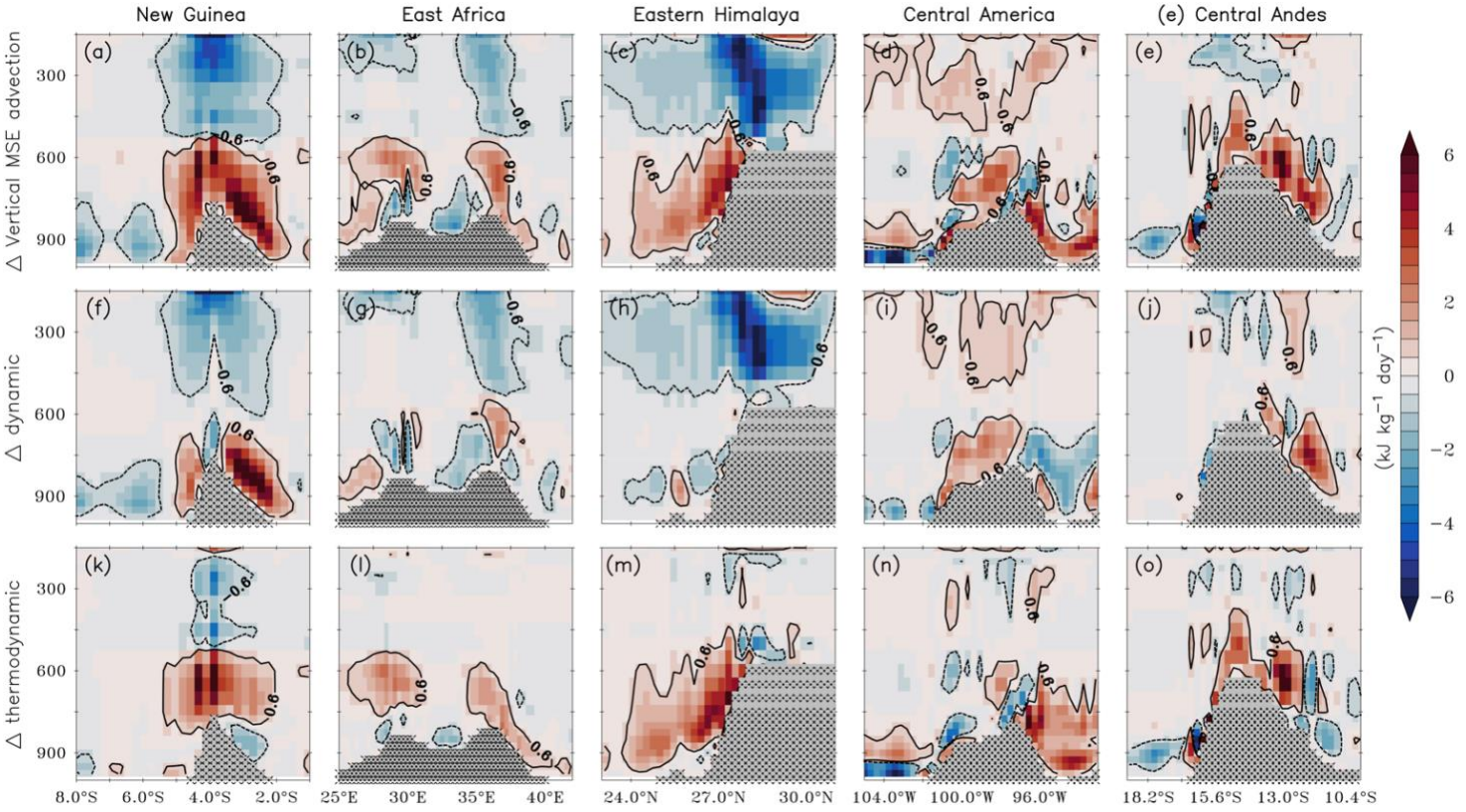

Fig. 8. Vertical structure of anomalous vertical moist static energy (MSE) advection in response to 4xCO_2. Shading and contour denote projected changes in vertical MSE advection over New Guinea, East Africa, Eastern Himalayas, Central America, and Central Andes. (a)-(e) Change in net vertical MSE advection, (f)-(j) change in the dynamical component of vertical MSE advection, and (k)-(o) change in a thermodynamical component of vertical MSE advection, respectively. Positive contours represent energy import and negative energy export.

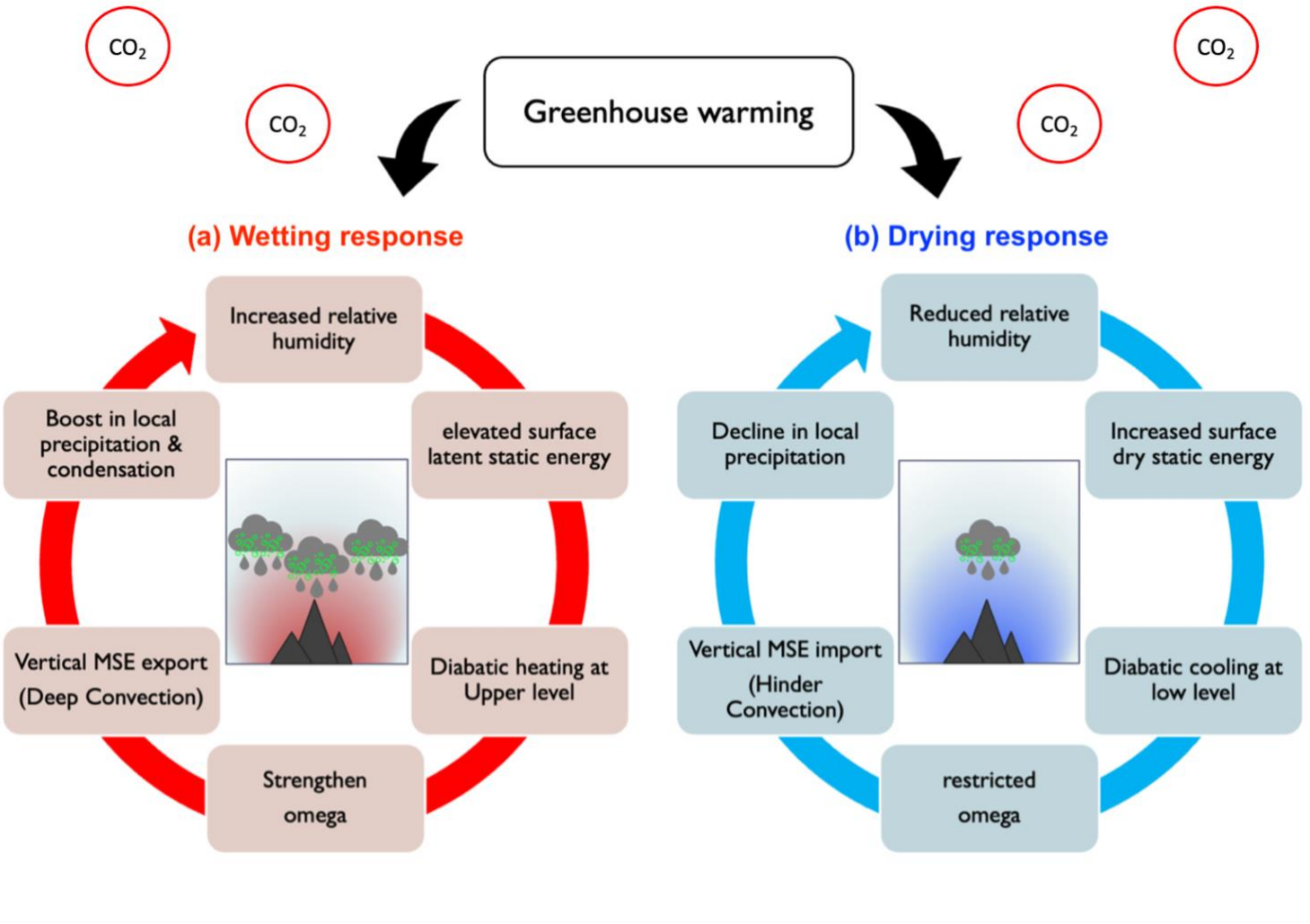

Fig. 9. Schematic representation of "Orographic moist-convection feedback mechanism" over low-latitude mountains.

(a) Wetting response:

Atmospheric relative humidity in the mountain terrain will increase due to greenhouse warming and favors a drop strengthen ascending motion in a humid climate through total diabatic heating. Simultaneously, vertical moist static energy export will feed ascending motion by deep convection. It boosts local precipitation and further contribute to the initial humidity.

(b) Drying response:

Atmospheric relative humidity in the mountain will reduce and this limited humidity weakens ascending motion through total diabatic cooling. Dry static energy contributes to low-level warming and dry conditions. Vertical moist static energy import will feed descending motion. Local precipitation decreases and initial humidity is further reduced as a result.

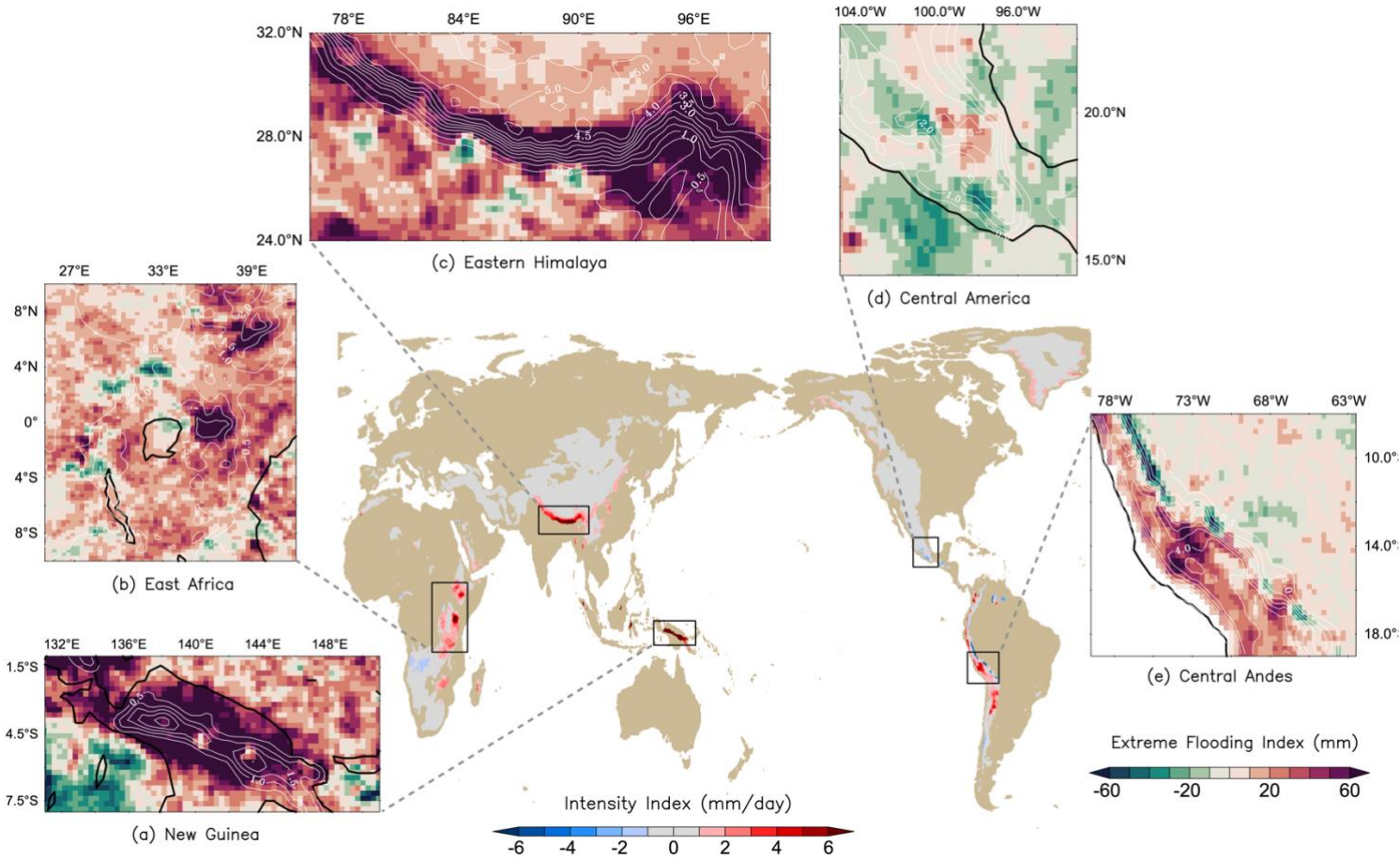

Fig. 10. Projected change in precipitation extremes over global mountain system in response to 4×CO_2. The center panel indicates extreme intensity index (SDII), and sub-panels (a)-(e) show the extreme flooding index (Rx5day). White contour shows an elevation orography of 0.5 km interval.